Original

Meinke, I.:

A Comparison of Simulated Clouds to ISCCP Data

In: Monthly Weather Review (2006) AMS

DOI: 10.1175/MWR3139.1

A Comparison of Simulated Clouds to ISCCP Data

INSA MEINKE*

GKSS, Institute for Coastal Research, Max-Planck-Strasse, Geesthacht, Germany

(Manuscript received 5 June 2003, in final form 4 July 2005)

ABSTRACT

An evaluation of the cloud parameterization scheme in the High-Resolution Regional Model (HRM) of the Deutscher Wetterdienst was conducted using data from the International Satellite Cloud Climatology Project (ISCCP). Uncertainties in the model and in the measurements were first quantified. Then, criteria for comparisons of simulated and measured data were chosen in order to identify model deficiencies. The simulated clouds were subsequently classified by their parameterization so model deficiencies could be easily attributed to a certain parameterization scheme. Following this evaluation, an overestimation of simulated mean cloud amount was identified as a deficiency of the HRM. The overestimation occurred mainly during the night and was due to an overprediction of subscale clouds at low-level emissivity heights. At medium-level emissivity heights during the day, the cloud amount is underpredicted. This leads to an underestimation of the diurnal cycle. These deficiencies were connected with the relative humidity parameterization used to characterize subscale cloudiness.

1. Introduction

Various international model intercomparisons show that cloud parameterization schemes pose a major source of uncertainties in numerical weather forecasts and climate predictions (e.g., Gates et al. 1999; Jacob et al. 2001; Ahrens et al. 1998; Klein and Jakob 1999; Nolte-Holube et al. 1996; Zhang et al. 2001). Differences between simulated and satellite-derived clouds may be caused by a number of factors, including 1) uncertainties in the measurements, 2) model-generated uncertainties that are not part of the cloud parameterization scheme, and 3) the way satellite data of surface-scanning radiometers are used to evaluate the vertical distribution of simulated clouds. To make sure the differences between model and measurements represent a deficiency of the cloud parameterization scheme in the model, the impact of these uncertainties has to first be considered (Meinke 2002).

The objective of this study is to carry out an evaluation of the cloud parameterization scheme in the High-Resolution Regional Model (HRM) using the International Satellite Cloud Climatology Project (ISCCP) data. As will be shown, an overestimation of simulated cloud amount in low-level emissivity heights and an underestimation of the cloud diurnal cycle are significant model deficiencies. Both are connected with the relative humidity parameterization.

2. Basis of the validation

a. Model domain and calculation period

The model domain comprises the northeastern part of the North Atlantic Ocean and northern, middle, and eastern Europe as shown in Fig. 1. Located in midlatitudes, this region is impacted by frontal cyclones and by subtropical high pressure systems. Most clouds in the area are connected with frontal cyclones. These are mostly stratiform clouds generated ahead of a warm front as warm air masses slide over cold air masses. Convection in the midlatitudes has a considerable diurnal and annual cycle over land with maxima during the day and summer and minima during the night and winter.

The period of interest is August–October 1995, dur-

* Current affiliation: Experimental Climate Prediction Center, Scripps Institution of Oceanography, University of California, San Diego, La Jolla, California.

Corresponding author address: Dr. Insa Meinke, Experimental Climate Prediction Center, Scripps Institution of Oceanography, University of California, San Diego, 9500 Gilman Dr., MC 0224, La Jolla, CA 92093-0224.
E-mail: imeinke@ucsd.edu

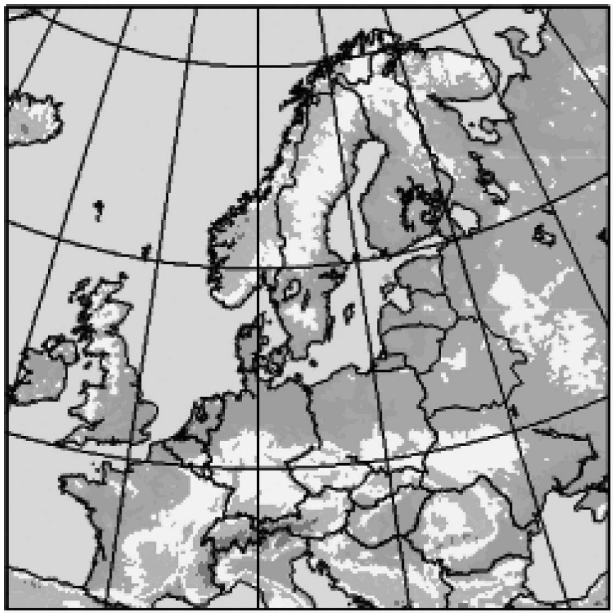

FIG. 1. Model domain.

ing the enhanced observational period of the Baltic Sea Experiment named the Pilot Study for Intensive Data Collection and Analysis of Precipitation (Isemer 1996). This time span requires the simulation of clouds with various origins: while in August the meteorological conditions are favorable for convection, in September and October the number of frontal cyclones increases (Meinke 2002).

b. The HRM

The HRM is a three-dimensional hydrostatic numerical model. The spherical coordinate system is rotated with the North Pole at 32.5°N and 170°W. Thus, the horizontal grid boxes in the model area are nearly equally spaced. The horizontal resolution of the HRM is 0.125° (~14 km). The model area consists 241 × 241 grid boxes. The atmosphere is discretized on 30 vertical model layers in a hybrid coordinate system. Surface pressure, horizontal wind components, temperature, water vapor, and cloud water are calculated by prognostic equations. The prognostic equations are solved in the interior of the model domain [Deutscher Wetterdienst (DWD) 1995]. On the lateral boundary of the model area, the values of all parameters agree with the lateral boundary condition used to initialize and drive the model. Grid-scale and convective clouds are simulated using the prognostic schemes of Kessler (1969) and Tiedtke (1989). The radiative budget is calculated by a delta two-stream approximation (Ritter and Geleyn 1992). For radiative transport simulations cloud fraction is set to 100% if grid-scale cloud liquid water has been calculated by the prognostic equations. Otherwise, subscale cloudiness is calculated by a relative humidity parameterization after Geleyn (1981). If the simulated relative humidity (RH) exceeds a critical value (RHC) of

$$\mathrm{RHC} = 0.95 - \mathrm{UC1} \times \sigma(1 - \sigma) \times [1 + \mathrm{UC2} \times (\sigma - 0.5)]$$

cloud cover is assumed. Here $\sigma = p/p_s$, where p_s is the surface pressure and p is the pressure of the respective model layer, and UC1 and UC2 are the respective empirical constants (UC1 = 0.8 and UC2 = 1.73). For the simulation of radiatively relevant convective cloud properties, the prerequisites for convection in the various layers have to be fulfilled. The subscale cloud fraction is a function of the instantaneous calculated RH and the RHC. The subscale cloud fraction is calculated by

$$\mathrm{CLC} = \mathrm{MAX}\left[0, \mathrm{MIN}\left(1, \frac{\mathrm{RH} - \mathrm{RHC}}{1 - \mathrm{RHC}}\right)\right]^2.$$

The radiatively relevant liquid water content of the subscale cloudiness in the HRM is set to 0.5% of the saturation humidity of each layer. For convective clouds it is set to 1% of the saturation humidity because it is assumed that the convective clouds have larger liquid water content. The forecast liquid water content of grid-scale cloudiness is reduced by 50%, otherwise the diurnal cycle of the near-surface temperature would be too low (DWD 1995). Besides cloud fraction and cloud liquid water content, the radiation scheme needs a cloud overlap assumption. The HRM follows the scheme of Tian and Curry (1989), which is a maximum random overlap assumption.

In this study the HRM is initialized and forced with boundary conditions of two different analyses, namely, the European Centre for Medium-Range Weather Forecasts (ECMWF) global analyses and the DWD EM3AN analyses. The HRM runs were carried out in forecast mode, with initialization every 24 h and boundary information every 6 h. Every 30 h the model is reinitialized. This ensures that the simulations are in close agreement with the data. To ameliorate the spinup effect, the first 6 h of each forecast were neglected in the analysis (Karstens et al. 1996). The evaluation is carried out for cloud amount, as it is a key variable for many other processes described by the cloud and radiation parameterization schemes. Cloud amount is the percentage of cloudy grid boxes in the model domain.

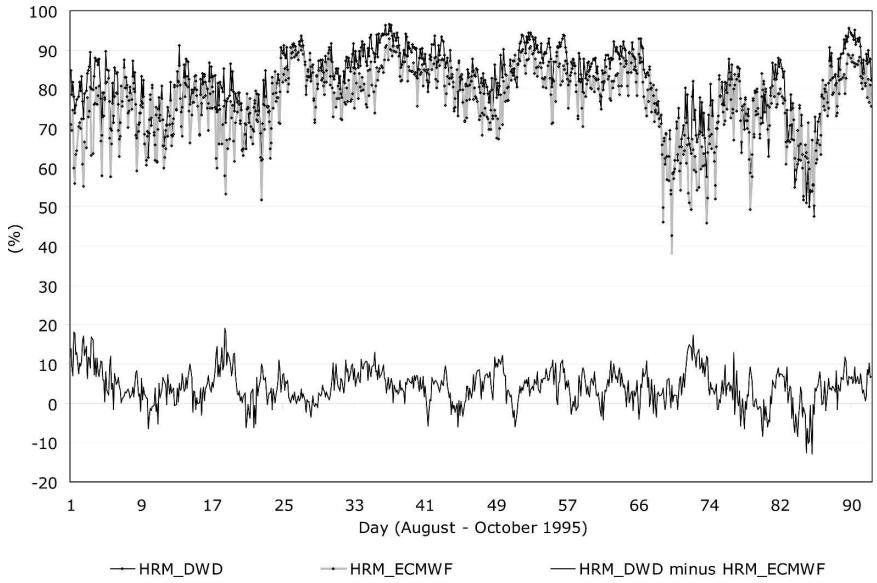

FIG. 2. Area means of cloud amount simulated by HRM initialized with DWD analyses and with ECMWF analyses and their differences (August–October 1995).

c. *The ISCCP data*

Data from ISCCP are used for the evaluation of the HRM cloud parameterization schemes. ISCCP has a cloud detection algorithm based on surface-scanning radiometers. It can be applied to polar-orbiting and geostationary satellites. The data processing has been carried out operationally since 1983 (e.g., Rossow et al. 1996). Surface-scanning radiometers have a temporal resolution that is two orders of magnitude higher than that of vertically sounding radiometers. The ISCCP-DX data used for this evaluation have the highest resolution of all ISCCP products (4–7 km, depending on the viewing angle). The satellites available over the area of interest during August–October 1995 were the National Oceanic and Atmospheric Administration (NOAA) satellites *NOAA-12*, *NOAA-14*, and *Meteosat-5*, operated by EUMETSAT. The data from their overpasses are accumulated in 3-hourly time slots. To reduce the data volume, one pixel with a resolution of the standardized field of view of the infrared radiometers is extracted every 25 to 30 km. Cloud parameters are derived using this reduced dataset. The cloud detection of ISCCP is based on two steps. First dynamical background values for cloud free situations are derived. Threshold tests for cloud detection are than carried out in the infrared and visible spectra using these background values. The cloud-top pressure is calculated by simulating the cloud-top temperature in a radiation transport model (Rossow 1989). Using temperature profiles from the Television Infrared Observation Satellite Operational Vertical Sounder the corresponding cloud-top pressure is determined.

3. Uncertainties within the HRM–ISCCP comparison

a. *Uncertainties regarding the model*

Uncertainties connected with the HRM that are not part of the atmospheric model and its parameterization can be caused by the data used to initialize and force the model (e.g., Downton and Bell 1988). Even small disturbances in the initial state can have major impacts on the quality of weather forecasts (Buizza 2000). Thus, an impact on the forecast is also likely if the forcing is replaced. The HRM was initialized and driven by the two different boundary conditions described above. To examine the sensitivity of the model to forcing, the cloud amount from August to October 1995 from two model runs with different forcing are compared (Fig. 2). There is an average difference of 4.22% between the cloud amounts of the two HRM runs (significance level at 99.9%). The standard deviation of the differences is 4.58%. This indicates that the simulation of cloud-relevant interactions and processes is sensitive to minor changes in the forcing. Over land surfaces, the mean difference of simulated cloud amount between the two model runs is 5.28% with a standard deviation of 5.19%. Over water surfaces it is smaller, with a mean difference of 2.58% and a standard deviation of 6.22%.

b. *Uncertainties regarding the cloud detection from satellite data*

Most of the uncertainties in satellite-derived cloudiness are due to assumptions of the cloud detection al-

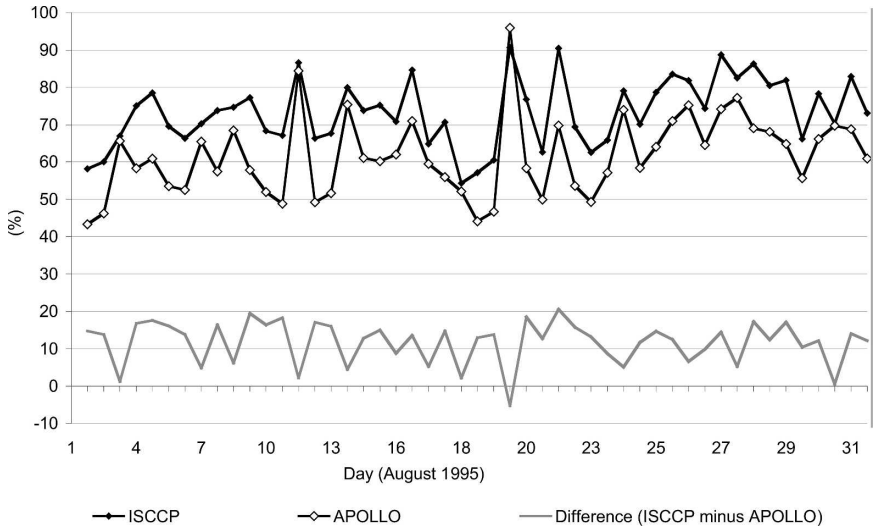

FIG. 3. Cloud amount of *NOAA-14* AVHRR data derived by the cloud detection algorithm of ISCCP and APOLLO and their differences (August 1995).

gorithm. To study the impact of applying various cloud detection algorithms, *NOAA-14* Advanced Very High Resolution Radiometer (AVHRR) data from August 1995 has been processed by the ISCCP cloud detection algorithm and by the AVHRR Processing Scheme over Clouds, Land and Ocean (APOLLO) algorithm (Saunders and Kriebel 1988). For comparison, the *NOAA-14* AVHRR data processed by the APOLLO algorithm has been sampled by the same method used for the ISCCP cloud detection (Fig. 3). Although both cloud detection algorithms have been applied to the same data, there is a statistically significant (level at 99%) average difference of 11.75% with a standard deviation of 5.69%. This indicates that the cloud detection algorithm applied to the satellite data is causing uncertainties. These differences and their standard deviations vary with surface type: over land surfaces the mean difference between ISCCP and APOLLO cloud amount is 23.51% with a standard deviation of 6.62%, whereas over water surfaces the mean difference between ISCCP and APOLLO cloud amount is only 0.92% with a standard deviation of 2.7%.

c. Ranges of uncertainty

Now the question is how to specify a range of uncertainty. In doing so, the notion is adopted that the considered quantity, say the monthly or seasonal mean cloudiness in a 3-month period, is a random variable. The random character originates not from the temporal variability, but from the process of generating the data. In the case of the simulated cloudiness, the randomness has its origin in the use of different initial conditions and boundary values for the same regional model. In the case of the satellite-derived cloudiness, the different realizations of the random variables are provided by the cloud detection algorithm used for deriving cloud properties from the radiances. The problem in both cases is that there are only a few samples of the random variables, which makes estimation rather cumbersome and inaccurate. Nevertheless, the little information available can be used to derive some, admittedly crude, estimates of uncertainty ranges.

As is commonly done, the concept of a confidence band is used. To formalize this, the random variable W is introduced. When there are n samples W_i of W, the mean value is estimated by

$$\mu = \frac{1}{n}\sum_{i=1}^{n} W_i$$

and the variance by

$$\sigma_w^2 = \frac{1}{n}\sum_{i=1}^{n} (W_i - \mu)^2.$$

Then the confidence interval α that on average contains α of all realizations W_i of W is given by

$$P[W \in (\mu - k\sigma_w; \mu + k\sigma_w)] = \alpha$$

with

$$k = S^{-1}\left(\frac{\alpha + 1}{2}\right),$$

where S denotes the distribution function of the normal distribution and P is the probability of the event given in brackets. Thus,

TABLE 1. Uncertainty ranges of ISCCP and APOLLO cloud detection results depending upon surface type.

Surface type	Uncertainty ranges
All surface types	16.28%
All land surfaces	32.58%
Ice surfaces	15.71%
Mountain surfaces (>1000 m)	26.53%
Water surfaces	1.28%

TABLE 2. Uncertainty ranges (at a level of 95%) for the processes generating the data (cloud amount).

	Simulated (HRM)	Satellite derived (ISCCP)	Combined range
All surface types	4.14%	16.28%	16.8%
Land surfaces	5.17%	32.58%	32.99%
Water surfaces	2.53%	1.28%	2.84%

$$\pm S^{-1}\left(\frac{\alpha+1}{2}\right)\sigma_w$$

is the uncertainty at a level of α. Thus, if $\alpha = 95\%$, then $k = S^{-1}(0.975)$ and the uncertainty is $\pm 1.96\sigma_w$. This is the standard approach (e.g., von Storch and Zwiers 1999). The problem is to estimate the unknown parameters μ and σ_w when only very few data are available.

To assess uncertainties in the HRM, two equivalent realizations were performed. This is the case of the randomness related to different analyses used to force the regional model. The two realizations (HRM initialized with ECMWF analyses and HRM initialized with DWD analyses, respectively) are denoted as W_1 and W_2, so

$$\mu = \frac{W_1 + W_2}{2} \quad \text{and}$$

$$\sigma_w^2 = \frac{1}{2}[(W_1 - \mu)^2 + (W_2 - \mu)^2]$$

$$= \frac{(W_1 - W_2)^2}{4}.$$

For calculation of all uncertainty ranges the level of $\alpha = 95\%$ is uniformly used. Hence, the uncertainty range of simulating cloud amount with the HRM $[k\sigma_{w(\mathrm{HRM})}]$ caused by changing the initialization and boundary values is about $\pm 4\%$ (Table 2). Over land the derived uncertainty range is about $\pm 5\%$. Over water the range of uncertainty is lower with a value of about $\pm 3\%$ (Table 2). In the other case, there is one regular realization for the 3 months (August–October 1995): the cloudiness derived with the ISCCP cloud detection algorithm (W_1) plus cloudiness derived with the cloud detection algorithm APOLLO for August 1995 (W_2). Since cloudiness has a distinct annual cycle, the time-limited APOLLO data cannot be used to estimate the seasonal mean (August–October), and it has to be set at $\mu = W_1$. However, it is proposed to use the APOLLO data to estimate the variance

$$\sigma_w^2 = \frac{1}{2}[(W_1 - W_1)^2 + (W_2 - W_1)^2]$$

and it is found that

$$\sigma_w^2 = \frac{(W_1 - W_2)^2}{2}.$$

Thus, the range of uncertainty caused by the cloud detection algorithms $[k\sigma_{w(\mathrm{SAT})}]$ derived as described above is about $\pm 16\%$ over all surface types (Tables 1 and 2). The range of the uncertainty varies with the surface type (Table 1): over land the range of uncertainty is about $\pm 33\%$; over water the range of uncertainty is much smaller with a value of about $\pm 1\%$ (Table 1). This shows that the cloud detection is most reliable over homogeneous surfaces like water. Over ice surfaces and mountains it is most uncertain (Table 1).

As previously mentioned, this is a very crude estimate of the uncertainty ranges. Even one additional sample would be helpful in arriving at more reliable estimates. However, even two samples are useful for estimating the inherent uncertainty.

d. Interpretation of the vertical information from radiances of surface-scanning radiometers

Uncertainties regarding the cloud-top pressure derived from radiances of surface-scanning radiometers are mostly caused by misinterpretation of the data. In spite of single clouds with well-defined cloud tops and large optical thickness, the measurements of clouds by surface-scanning radiometers are mostly based on mixed signals. These mixed signals can be caused in different ways: 1) A cloud with low optical thickness overlies another cloud with a higher optical thickness or the surface. The derived cloud-top pressure represents the emissivity height of this multilayered cloud or the emissivity height of the low optical thickness cloud and the surface, respectively. 2) Clouds with diffused cloud tops are another source for mixed signals. The optical thickness of these clouds slowly increases from the physical cloud top downward. In these cases, the derived cloud-top pressure represents the emissivity height of the whole radiating cloud column. 3) Subscale clouds cause uncertainties in measured cloud-top height as the radiative properties of the subjacent layer

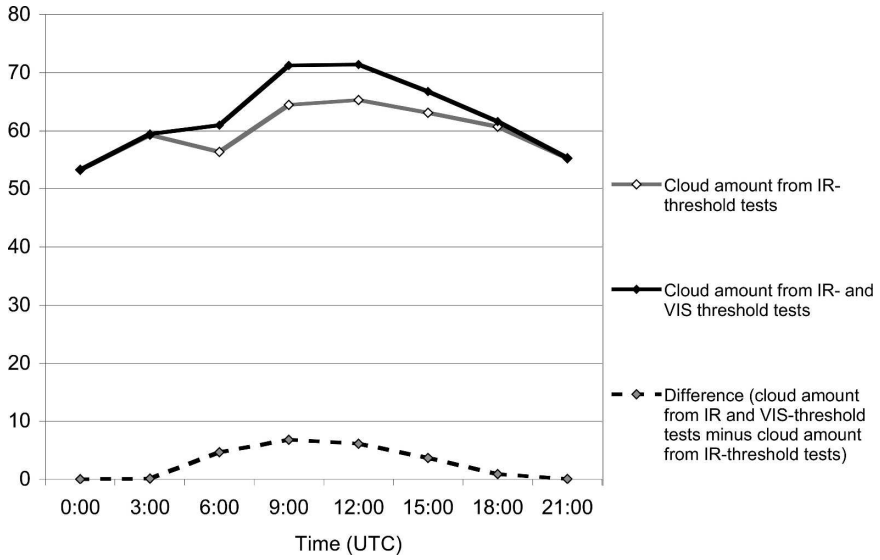

FIG. 4. Cloud amount detected by ISCCP cloud detection algorithm on the basis of radiances of various spectra (temporal averaged area means).

(cloud or surface) affect the signal measured by surface-scanning radiometers.

Analyses of rawinsonde data (Wang et al. 2000) show that the proportion of multilayered clouds to all clouds is about 42%. Also, analyses of the Second Stratospheric Aerosol and Gas Experiment data (Liao et al. 1995a,b) indicate that 30%–40% in winter and 40%–50% in summer of all midlatitude clouds are comprised of clouds with diffused cloud tops. Hence, it is quite possible that a measured cloud in the midlatitudes meets one of these three criteria (low optical thickness/multilayered, diffused top, or subscale). Cases in which the derived cloud-top pressure is identical to the physical cloud-top height are quite rare. Summarizing these aspects, the cloud-top pressure derived by surface-scanning radiometers usually represents the emissivity height of a cloud column.

e. Availability of radiances in the visible spectrum

Another bias in cloud detection from satellite data is caused by the varying availability of radiances in the visible spectrum. As the visible spectrum is not available during the night there is a systematic difference in cloud detection between daytime and nighttime. This is indicated by the difference in cloud detection on the basis of various spectra (Fig. 4). If the cloud detection has been carried out on the basis of radiances in the visible and infrared spectra, the cloud amount detected is significantly higher than if the cloud detection has been carried out solely on the basis of infrared radiances. The mean difference between the cloud detection from visible plus infrared and solely from the infrared is 2.78%. The small standard deviation of 0.9% indicates the systematic origin of the differences.

4. Criteria and requirements for the comparison

Three sources of uncertainties have to be taken into account for a model validation: initial and boundary conditions, the cloud detection algorithm, and misinterpretation of the cloud-top pressure derived from radiances of surface-scanning radiometers. The availability of the visible spectrum also has an impact on cloud detection. However, this introduces systematic errors, not uncertainties.

The combined range of the first two uncertainties U caused by the model $[k\sigma_{w(\mathrm{HRM})}]$ and the satellite data $[k\sigma_{w(\mathrm{SAT})}]$ is given by

$$U = \sqrt{[k\sigma^2_{w(\mathrm{HRM})} + k\sigma^2_{w(\mathrm{SAT})}]}.$$

Hence, for cloud amount the combined range of mean uncertainty is about ±17% over all surface types, about ±33% over land surfaces, and about ±3% over water surfaces (Table 2).

To identify deficiencies of the model by comparing the model output with satellite-derived data, two criteria have to be fulfilled (Table 3). First, the differences between model and data need to be statistically significant. Otherwise they might be random. Second, the magnitudes of the differences between model and data have to exceed the combined estimated ranges of uncertainty as in Table 2. When both of theses criteria are

TABLE 3. Criteria and requirements for comparability.

Criteria and requirements	Use
Differences of simulated and measured data have to be statistically significant	Differences do not appear at random
Magnitude of the differences has to exceed the combined uncertainty ranges	Difference is not mainly caused by these uncertainties
Calculation of emissivity levels of the simulated cloud columns	Comparability of simulated and satellite-derived vertical cloud distribution
Cloud detection on the basis of infrared spectra	Homogeneity in the cloud detection, no systematic errors

met, the differences between the simulated and measured data can be identified as model deficiencies. In comparisons of simulated and satellite-derived cloud-top pressure, it has to be taken into account that the surface-scanning radiometer-derived values represent the emissivity height of a vertical cloud column, not the exact physical cloud-top height. Hence, to fulfill the requirements for comparability with the ISCCP data, the emissivity heights of the simulated cloud columns have to be calculated (Table 3).

To avoid systematic errors caused by the changing availability of radiances in the visible spectrum, the cloud detection of ISCCP used for the validation has been carried out solely on the basis of the infrared spectrum.

5. Identification of deficiencies in the model

For comparison of simulated and satellite-derived cloud amounts, the simulated values were only taken into account if ISCCP data were available at the same time and in the same grid box. To avoid inconsistencies caused by the model boundary, the values of the eight outer model grid boxes were omitted (Fig. 5).

a. Representation of cloud amount

The differences between cloud amounts of both HRM runs and the ISCCP data are statistically significant. The mean difference between the HRM initialized with DWD analyses and ISCCP is 17.5%. Between the HRM initialized with ECMWF analyses and ISCCP, the mean difference is smaller, with a value of 13.3%. Thus, only the difference between the HRM initialized with DWD analyses and ISCCP exceed the combined uncertainty ranges of ±17%. However, over water surfaces where cloud detection from satellite data is most certain, the magnitudes of the mean differences between both HRM runs and the ISCCP data exceed the combined uncertainty ranges of ±3% and are statistically significant. Because both comparison criteria are easily met over water surfaces, it is clear that the HRM overpredicts simulated cloud amount over water. In fact, the same tendency was present over land surfaces, although there is the higher range of uncertainty over land surfaces, because of the higher uncertainty of cloud detection from satellite data over surfaces with

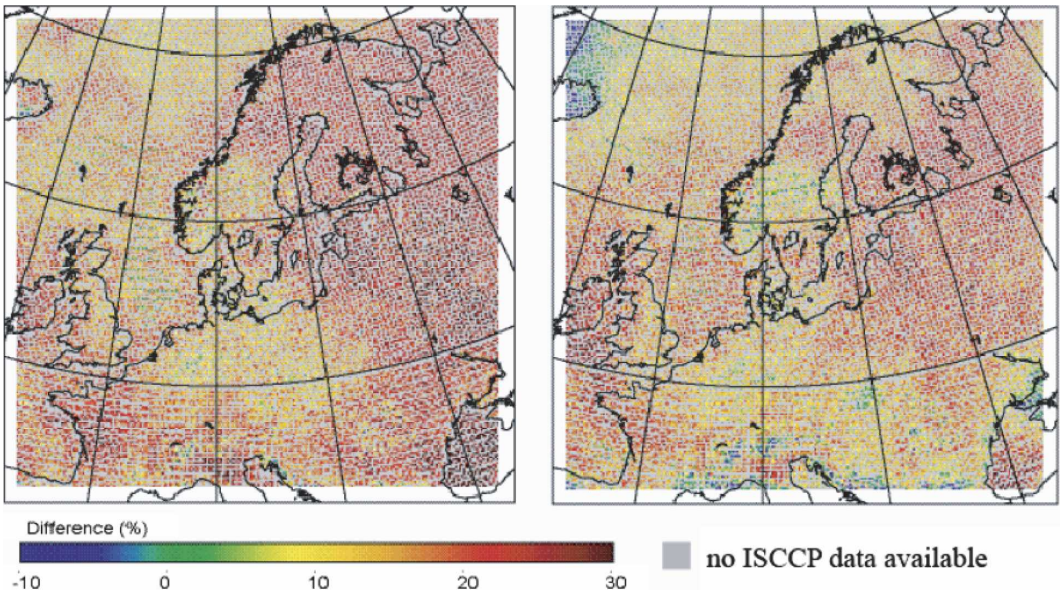

FIG. 5. Mean differences in cloud amount: August–October 1995 (left) HRM, initialized with DWD analyses minus ISCCP, and (right) HRM initialized with ECMWF analyses minus ISCCP.

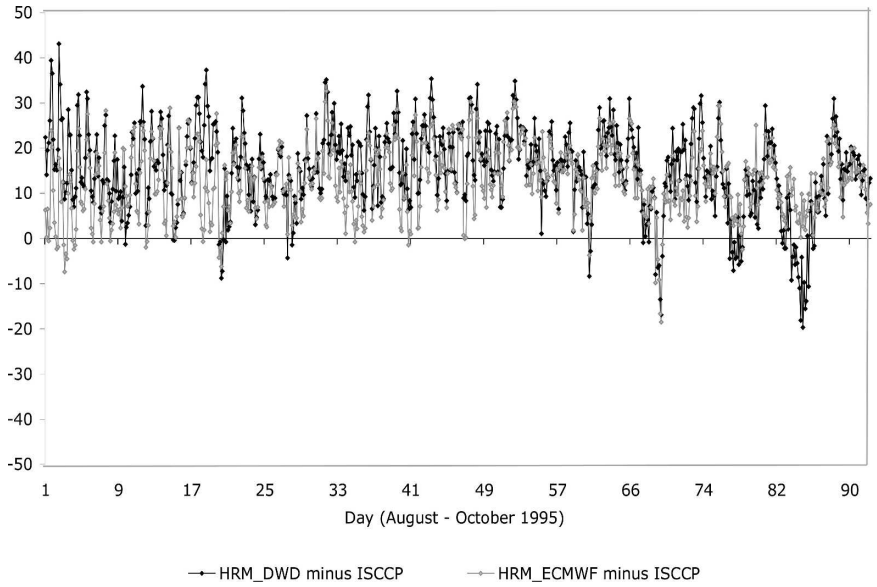

FIG. 6. Temporal variations of differences between simulated (HRM) and satellite-derived (ISCCP) cloud amounts (August–October 1995 area means over water surfaces).

inhomogeneous radiative properties. Figure 6 shows the temporal distribution of the differences over water surfaces (area means) between simulated and measured cloud amount. Regardless of the initial and boundary conditions, the differences have a high temporal variability. To find explanations for this variability, the diurnal cycle of cloud amounts was also examined (Fig. 7). Relative to the diurnal cycle of cloud amount derived from the ISCCP data, the diurnal cycle of the simulated cloud amount was too small (Fig. 7). This is independent of the initial condition of the HRM runs. Compared with ISCCP, both model runs (HRM-DWD and HRM-ECMWF) show large overestimations of the cloud amount, especially during the nighttime.

Summarizing this part of the validation there are two main results. 1) A model deficiency has been identified regarding the simulation of cloud amount. This deficiency is expressed by an overestimation of the simu-

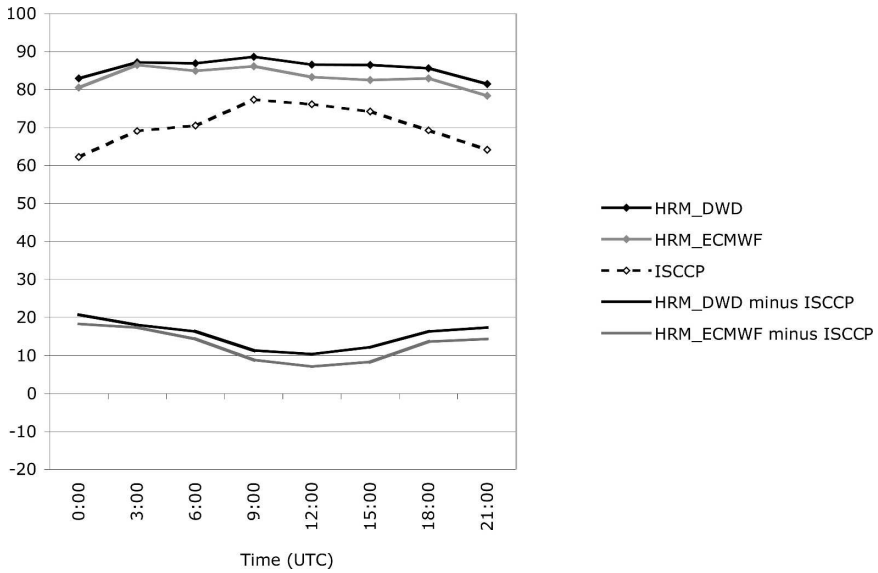

FIG. 7. Diurnal cycle of cloud amount and differences between HRM and ISCCP (August–October 1995 temporal averages of area means over water surfaces).

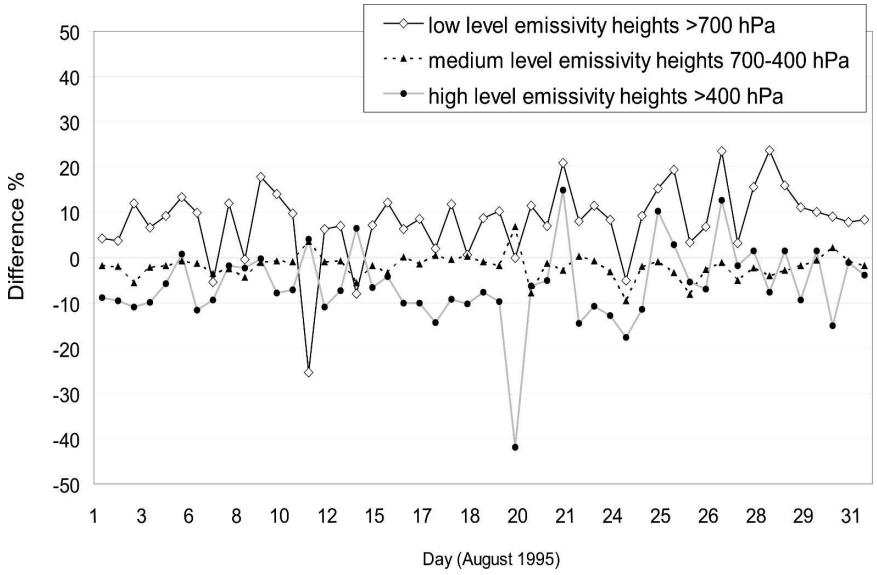

FIG. 8. Differences between ISCCP and APOLLO cloud amounts (ISCCP minus APOLLO) in cloud amount within low, medium, and high emissivity levels.

lated cloud amount in mean. 2) Appearing mainly during nighttime, the deficiency is due to an underestimation of the simulated diurnal cycle of cloudiness.

b. Representation of clouds on emissivity levels

Again, the emissivity levels of the simulated cloud columns have to be calculated to be comparable to the satellite-derived cloud-top pressure. The emissivity level is the pressure level whose corresponding temperature is the same as the brightness temperature of the vertical cloud column. The brightness temperature of the simulated vertical cloud column was calculated using the delta eddington approximation (Wiscombe 1977; Slingo 1989; Slingo and Schrecker 1982). As the calculation of cloud properties in the HRM is based on the center of each model layer, 30 emissivity levels must be calculated. The thickness of these emissivity levels varies between 10 and 60 hPa according to the chosen hybrid coordinate system.

To estimate the uncertainty of the satellite-derived cloud amount in emissivity levels, comparisons between ISCCP and APOLLO were conducted. APOLLO only distinguishes three levels of emissivity heights: low >700 hPa, medium 700–400 hPa, and high <400 hPa. For comparison with APOLLO cloud amounts in low-, medium-, and high-level emissivity heights, the ISCCP emissivity heights were subdivided into the same classes. Figure 8 shows the differences between ISCCP and APOLLO cloud amounts within the three different classes of emissivity heights. The largest difference, 8.11%, occurs for cloud amounts within the low-level emissivity heights. Second largest is the difference of −6.14% for the cloud amounts high-level emissivity heights. The lowest differences, 1.94%, occur for cloud amounts within the medium-level emissivity heights.

Additionally, the simulated cloud amounts within the 30 emissivity levels of both model runs are compared in order to estimate uncertainties caused by using different analyses as forcing of the HRM. Figure 9 shows the mean differences between cloud amounts in various emissivity heights of the two model runs. As the signs of the differences are changing within the vertical distribution, the root-mean-square differences were calculated. Afterward the differences were integrated referring to the emissivity level classes used by APOLLO.

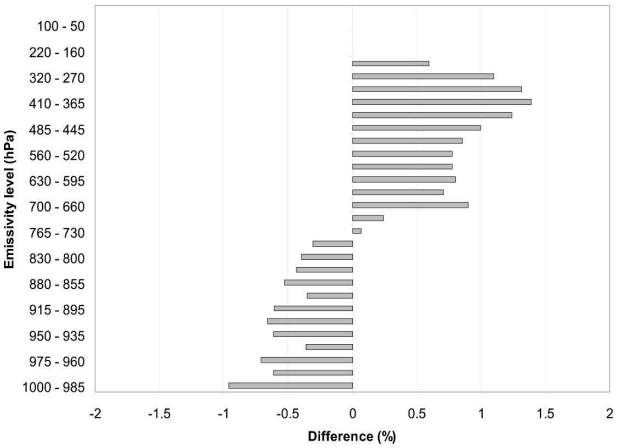

FIG. 9. Differences between HRM-DWD minus HRM-ECMWF in cloud amount (August–October 1995 mean).

TABLE 4. Uncertainty ranges and differences within emissivity heights (cloud amount).

Emissivity levels	Uncertainty range HRM	Uncertainty range ISCCP	Combined uncertainty range	Diff HRM-DWD − ISCCP	Diff HRM-ECMWF − ISCCP
Low (>700 hPa)	6.11%	11.24%	12.79%	15.6%	21.83%
Medium (700–400)	8.28%	2.69%	8.71%	−3.6%	−12.04%
High (<400)	2.95%	8.51%	9.01%	7.98%	3.06%

The largest difference occurs for cloud amounts in the medium-level emissivity height with 8.45%. In the low-level emissivity height the difference between cloud amounts of the two model runs is 6.84%. In high-level emissivity heights, the difference of cloud amount is smaller with a mean value of 3.01%. Table 4 shows the ranges of uncertainty of the simulated and satellite-derived data and their combined uncertainty ranges. All ranges are calculated as previously described in sections 3c and 4. The largest combined uncertainty range is about ±13% for cloud amounts in the low-level emissivity heights. The combined ranges of uncertainty for clouds in the medium- and high-level emissivity heights are about ±9% each.

In Fig. 10 the differences between simulated and satellite-derived cloud amount are shown. The signs of the differences change within the emissivity levels. Thus, as before the root-mean-squared differences were calculated. The highest level of significance (99%) is within the differences between simulated and satellite-derived cloud amounts in the low-level emissivity heights. Referring to the low emissivity heights of APOLLO, the differences of both model runs and ISCCP exceed the combined range of uncertainty of about ±13% (see Table 4). This shows that the HRM overpredicts cloud amounts in low-level emissivity heights (see Fig. 10). Additional evidence that the claimed overestimation of the simulated low-level cloud amount is not caused by an underestimation of the ISCCP cloud amount is that the APOLLO-retrieved cloud amount in low emissivity heights is even less frequent than the ISCCP-retrieved cloud amount in low-level emissivity heights.

For cloud amounts in the medium-level emissivity height, only the differences between one of the two model runs and ISCCP exceed the combined range of uncertainty of ±9% (see Table 4). The differences of cloud amounts in high-level emissivity heights between the HRM runs and ISCCP are not statistically significant and they do not exceed the combined range of uncertainty. Therefore, differences between HRM and ISCCP cloud amounts in the medium- and high-level emissivity heights cannot definitively be identified as model deficiencies.

The comparison of cloud distribution on emissivity heights shows that the pronounced overestimation of overall cloud amount during nighttime is caused by simulated clouds in the low-level emissivity heights (Fig. 11, left). During the daytime, the overall overestimation of the simulated cloud amount is smaller than during nighttime, because in combination with the negative differences of the HRM and ISCCP in the medium-level cloudiness the vertical integration of all differences leads to a smaller difference in total cloud amount, especially during the day (Fig. 11, right).

To summarize, the simulated cloud amount in low-level emissivity heights mainly causes the overestimation of all simulated cloud amounts; this overestimation occurs mainly during the night; the overall smaller differences between simulated and measured cloud amount during daytime are mainly caused by the negative differences between HRM cloud amounts minus ISCCP cloud amounts in the medium-level emissivity height. When vertically integrated, this compensates for the overestimation of simulated cloud amount in the low-level emissivity height.

6. Assigning model deficiencies to a certain cloud parameterization scheme

After identifying the deficiencies within the HRM regarding the simulation of cloud amount, one cannot specify which part of the cloud parameterization is

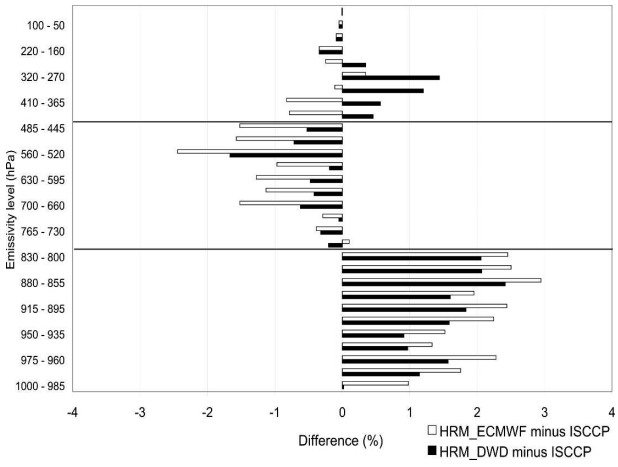

FIG. 10. Differences between simulated (HRM) and satellite-derived (ISCCP) cloud amounts on emissivity levels (August–October 1995 mean).

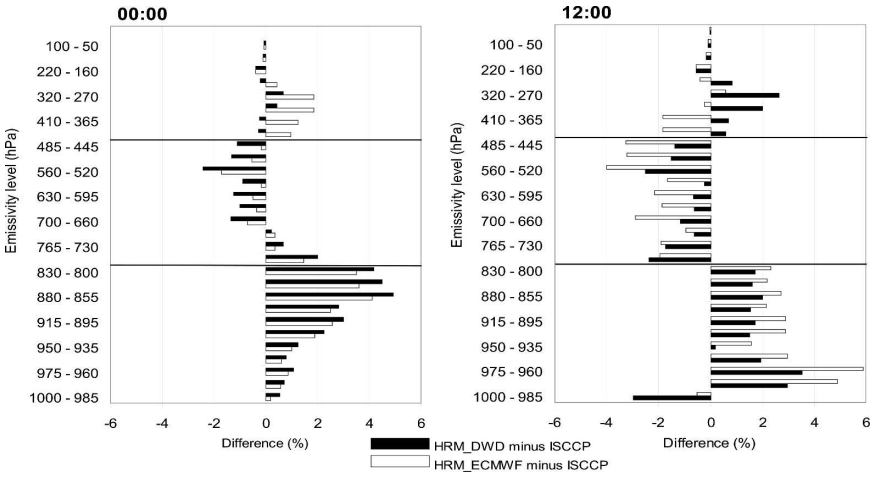

FIG. 11. Diurnal variation of differences between simulated and satellite-derived cloud amounts on emissivity levels (August–October 1995 mean).

causing deficiencies. Thus, in the next step of the evaluation the deficiencies are assigned to a certain cloud parameterization. This is achieved by classifying the simulated clouds according to their parameterization. The emissivity levels of simulated clouds represent a mixed signal of various radiative cloud properties in the vertical cloud column. In the HRM, the radiative cloud properties causing these mixed signals are parameterized diagnostically. Within this parameterization the results of the bulk scheme (Kessler 1969) and the convection scheme (Tiedtke 1989) are used to calculate the radiative cloud properties within the relative humidity parameterization (Geleyn 1981; see also section 2b). According to this parameterization, three different cloud types cause the mixed signal of the simulated cloud column: the grid-scale clouds, convective clouds, and subscale stratiform clouds. To assign the deficiencies to a certain parameterization scheme these cloud types were separated and emissivity levels were calculated for each type. Afterward the frequency distributions of these clouds on the emissivity heights are compared with the ISCCP data. In Fig. 12 the vertical distribution for the simulated cloud amounts with different parameterizations are shown along with the ISCCP data. The overestimation of cloud amount in the low-level emissivity height can be clearly assigned to subscale cloudiness. Even the single frequencies of the convective and the subscale stratiform clouds are higher than the cloud amount from the ISCCP dataset. Comparisons of the diurnal cycle indicate that subscale

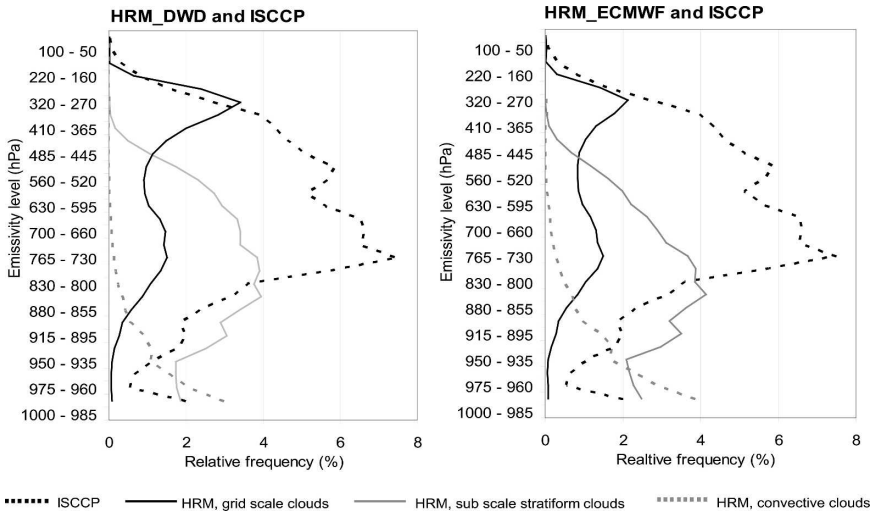

FIG. 12. Distribution of simulated clouds classified regarding their parameterization and ISCCP clouds on emissivity levels (August–October 1995 mean).

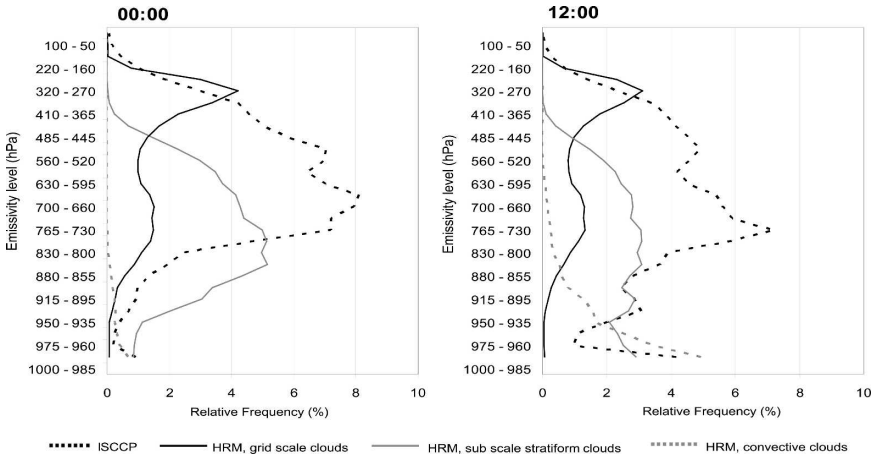

FIG. 13. Distribution of simulated clouds classified regarding their parameterization and ISCCP clouds on emissivity levels at 0000 and 1200 UTC (August–October 1995 mean).

stratiform clouds are the main cause for the overestimation of cloud amounts in the low-level emissivity heights during nighttime (Fig. 13, left). At midnight, the subscale stratiform cloud amount on its own is higher than the cloud amount of the ISCCP dataset. The subscale convective cloud amount has a significant diurnal cycle with a minimum at midnight and a maximum at noon. In contrast to the high overestimation of convective clouds in the low-level emissivity heights, there is nearly a complete absence of convective clouds in the medium-level emissivity heights.

7. Approaches for improved cloud simulations

Separating the simulated clouds according to their parameterization showed that the main part of the model deficiencies was caused by subscale cloudiness. These deficiencies in the HRM can be attributed to the relative humidity parameterization that defines subscale cloudiness. Two possible sources follow: 1) The deficiencies can be connected with the empirical factors of the relative humidity parameterization. These factors are a pressure-dependent threshold for calculating the subscale cloudiness and a factor for calculating the liquid water content, which is crucial for calculating the cloud fraction. 2) The deficiencies can be connected with the prognostic parameters in the relative humidity parameterization. Initializing the HRM every 24 h and giving boundary information every 6 h keep the prognosis of water vapor, pressure, temperature, and cloud water close to the measured state of these variables. Therefore, it is more probable that the deficiencies of the HRM are connected with the empirical part of the relative humidity parameterization. Nevertheless, it is ultimately important to also evaluate the water vapor and temperature profile. If the simulation of these prognostic variables had no deficiency, the empirical factors of the relative humidity parameterization would have to be adjusted to the measurements.

8. Discussion and conclusions

The presented comparison of simulated and satellite-derived clouds incorporates crucial requirements for a reliable evaluation: consideration of uncertainties regarding the model as well as the data, comparability of simulated and satellite-derived data, and isolation of the deficiency sources. The uncertainty ranges are estimated using the concept of confidence bands. For this purpose equivalent realizations of the process generating the data (simulation and measurement) are needed to make the estimation of the uncertainty range accurate. In the presented case only two realizations of the simulated and satellite-derived cloud amounts were available. Thus, the estimated range of uncertainty is not as precise as it could be with more equivalent realizations available. This as well concerns the comparability criterion referring to the combined uncertainty range. Nevertheless, even this crude estimate is useful for considering the inherent uncertainty. Also, if the uncertainty range of the measurements is too large, real deficiencies of the model might not be recognized. In this case, data received by another source of measurement might be helpful. Another option would be a data assimilation procedure to produce quantitative results on the model errors. However, the strategy shown is a fast way to validate a model by simple comparisons with measurements.

In the example shown here, the smallest uncertainty range was over water surfaces. This was mainly caused by the cloud detection from satellite data, which is most accurate over homogeneous surfaces. In the regional

atmospheric model HRM-simulated mean cloud amount is over predicted. This overprediction occurs mainly during the night. This is due to a deficiency in the HRM regarding the simulation of a proper diurnal cycle of cloudiness. As both model runs show the same behavior, this does not depend on the large-scale initial and boundary conditions.

To compare the simulated and satellite-derived vertical cloud structure, emissivity heights of the simulated clouds were calculated. These emissivity heights provide information on the vertical distribution of simulated clouds comparable to the satellite-derived cloud-top pressure. The comparisons show that the overestimation of all simulated clouds is caused by an overprediction of cloud amounts in low-level emissivity heights. Classifying the simulated clouds by parameterization, the overestimation of cloud amounts in the low-level emissivity heights was attributed to the relative humidity parameterization for subscale cloudiness. Thus, to improve the prediction of cloud amounts simulated by the HRM, changes in the relative humidity parameterization are most reasonable and promising. Some small modifications to this parameterization were suggested. It is ultimately important, however, to also evaluate the water vapor and temperature profile in order to avoid unrealistic adjustment of the relative humidity parameterization.

Acknowledgments. I thank Ehrhard Raschke for many valuable discussions and Hans von Storch for contributing to the statistics. I also thank William Rossow, John Roads, Burkhardt Rockel, Rolf Stuhlmann, George Tselioudis, Sarah Zedler, and the GCSS working group on extratropical layer clouds for important discussions.

REFERENCES

Ahrens, B., U. Karstens, B. Rockel, and R. Stuhlmann, 1998: On the validation of the atmospheric model REMO with ISCCP data and precipitation measurements using simple statistics. *Meteor. Atmos. Phys.,* **68,** 127–142.

Buizza, R., 2000: Chaos and weather prediction. ECMWF Int. Rep. 01/2000, 41 pp.

Downton, R., and R. Bell, 1988: The impact of analysis differences on a medium range forecast. *Meteor. Mag.,* **117,** 279–285.

DWD, 1995: Dokumentation des EM/DM Systems. DWD 06/1995, 234 pp.

Gates, L., and Coauthors, 1999: An overview of the results of the Atmospheric Model Intercomparison Project (AMIP I). *Bull. Amer. Meteor. Soc.,* **80,** 29–55.

Geleyn, J., 1981: Some diagnostics of the cloud/radiation interaction in ECMWF forecasting model. *Proc. ECMWF Workshop on Radiation and Cloud Radiation Interaction in Numerical Modeling*, Reading, United Kingdom, ECMWF, 135–162.

Isemer, H., 1996: Weather patterns and selected precipitation records in the PIDCAP period, August to November 1995. GKSS Ext. Rep. 55, 92 pp.

Jacob, D., and Coauthors, 2001: A comprehensive model intercomparison study investigating the water budget during the BALTX-PIDCAP period. *Meteor. Atmos. Phys.,* **77,** 17–43.

Karstens, U., R. Nolte-Holube, and B. Rockel, 1996: Calculation of the water budget over the Baltic Sea catchment area using the regional forecast model REMO for June 1993. *Tellus,* **48A,** 684–692.

Kessler, E., 1969: *On the Distribution and Continuity of Water Substance in Atmospheric Circulations. Meteor. Monogr.,* No. 32, Amer. Meteor. Soc., 84 pp.

Klein, S., and C. Jakob, 1999: Validation and sensitivities of frontal clouds simulated by the ECMWF model. *Mon. Wea. Rev.,* **127,** 2514–2531.

Liao, X., W. Rossow, and D. Rind, 1995a: Comparison between SAGE II and ISCCP high-level clouds. Part 1: Global and zonal mean cloud amounts. *J. Geophys. Res.,* **100,** 1121–1135.

——, ——, and ——, 1995b: Comparison between SAGE II and ISCCP high-level clouds. Part 2: Locating cloud top. *J. Geophys. Res.,* **100,** 1135–1147.

Meinke, I., 2002: Zur validierung der wolkenparametrisierung des regionalmodells HRM mit satellitendaten des ISCCP—Entwicklung und anwendung einer methode (Validating the cloud parameterization of the regional model HRM with ISCCP satellite data—Development and application of a method.). GKSS Ext. Rep. 2002 (19), 137 pp.

Nolte-Holube, R., U. Karstens, D. Lohmann, B. Rockel, and R. Stuhlmann, 1996: Regional scale atmospheric and hydrological modeling: Results and validation for the Baltic Sea and Weser catchments. GKSS Ext. Rep. 96 (54), 38 pp.

Ritter, B., and J.-F. Geleyn, 1992: A comprehensive radiation scheme for numerical weather prediction models with potential application in climate simulations. *Mon. Wea. Rev.,* **120,** 303–325.

Rossow, W., 1989: Measuring cloud properties from space: A review. *J. Climate,* **2,** 201–213.

——, A. Walker, and M. Roiter, 1996: International Satellite Cloud Climatology Project (ISCCP) documentation of new cloud datasets. WMO/TD-737, 115 pp.

Saunders, R., and K. Kriebel, 1988: An improved method for detecting clear sky and cloudy radiances from AVHRR data. *Int. J. Remote Sens.,* **9,** 123–150.

Slingo, A., 1989: A GCM parameterization for the shortwave radiative properties of water clouds. *J. Atmos. Sci.,* **46,** 1419–1427.

——, and H. Schrecker, 1982: On the shortwave radiative properties of stratiform water clouds. *Quart. J. Roy. Meteor. Soc.,* **108,** 407–426.

Tian, L., and J. Curry, 1989: Cloud overlap statistics. *J. Geophys. Res.,* **94,** 9925–9935.

Tiedtke, M., 1989: A comprehensive mass flux scheme for cumulus parameterization in large-scale models. *Mon. Wea. Rev.,* **117,** 1779–1800.

von Storch, H., and F. Zwiers, 1999: *Statistical Analysis in Climate Research.* Cambridge University Press, 484 pp.

Wang, J., W. Rossow, and Y. Zhang, 2000: Cloud vertical structure and its variations from a 20-yr global rawinsonde dataset. *J. Climate,* **13,** 3041–3055.

Wiscombe, W., 1977: The Delta-Eddington approximation for a vertically inhomogeneous atmosphere. NCAR Tech. Note NCAR/TN-121*STR, 66 pp.

Zhang, Y., B. Rockel, R. Stuhlmann, R. Hollmann, and U. Karstens, 2001: REMO cloud modeling: Improvements and validation with ISCCP DX data. *J. Appl. Meteor.,* **40,** 389–408.